PTAFR Exaggerates Microglia-Mediated Microenvironment via IL10-STAT3 Signaling: A Novel Perspective on Potential Biomarker and Target for AD Diagnosis and Treatment

Junxiu Liu (15804086989@163.com)
China Medical University https://orcid.org/0000-0003-4559-8854

Linchi Jiao
China Medical University

Xin Zhong
China Medical University

Weifan Yao
China Medical University

Ke Du
China Medical University

Senxu Lu
China Medical University

Yuqiang Wu
China Medical University

Tianxin Ma
China Medical University

Junhui Tong
China Medical University

Mingyue Xu
China Medical University

Wenjuan Jiang
China Medical University

Yubao Wang
Liaoning Medical Diagnosis and Treatment Center

Miao He
China Medical University

Wei Xin
The first Affiliated Hospital of China Medical University

Mingyan Liu
China Medical University

Research Article

Keywords: PTAFR, biomarkers, microglia, microenvironment, Alzheimer's disease

Posted Date: June 21st, 2021

DOI: https://doi.org/10.21203/rs.3.rs-625756/v1

Abstract

Background: Early diagnosis and effective intervention become the key points for delaying Alzheimer's progression. Therefore, we aim to find new biomarkers for early diagnosis of Alzheimer (AD) by bioinformatics, and to reveal the possible mechanisms.

Methods and results: GSE1297, GSE63063, and GSE110226 in the GEO database were used to screen out the differentially highly expressed genes. We found out a potential biomarker PTAFR differentially highly expressed in the brain tissue, peripheral blood and cerebrospinal fluid of AD patients. Furthermore, we found higher PTAFR level in the plasma and brain tissues of APP/PS1 mice. Simultaneously, it was uncovered that PTAFR mediated the inflammatory response to exaggerate microenvironment specially mediated by microglia through the IL10-STAT3 pathway. In addition, we also found PTAFR was a possible target for some anti-AD compounds such as EGCG, donepezil, curcumin, memantine, and Huperzine A.

Conclusions: PTAFR was a potential biomarker for early AD diagnosis and treatment correlated with microglia-mediated microenvironment, and an important possible target to make novel strategy for clinical treatment and new drug discovery in AD.

Introduction

As a neurodegenerative disease closely related to age, Alzheimer's Disease (AD) seriously endangers the lives of the elderly[1, 2]. Cognitive deficits, memory loss, and language dysfunction were the major clinical characteristics of AD[3]. And the hallmark pathophysiological changes include senile plaques formed by Aβ deposition in the brain, and the neurofibrillary tangles cause by tau hyperphosphorylation, gliosis and etc[4, 5]. Once clinical symptoms occur, it is hard to reverse the procession[6, 7]. Therefore, early diagnosis and treatment are overwhelmingly significant for delaying the progression of AD.

The clinical methods commonly used for AD diagnosis mainly include MMSE score, 18FDG-PET, CT or MRI scanning, EEG and biomarkers in cerebrospinal fluid of AD patients nowadays. Despite MMSE score is a convenient and low-cost method, it is usually used for screening moderate to severe AD. ^{18}FDG-PET, CT or MRI scanning are often used for excluding other diseases through imaging and improving the reliability of AD diagnosis, which are inconvenience and high-cost. EEG is insensitive for detecting early AD. And the changes of biomarkers in cerebrospinal fluid of AD patients seem more believable for AD diagnosis, but the sample collection is invasive, compared with those of other body fluids such as blood or urine [7, 8]. Therefore, finding out potential biomarkers with high specificity in the blood is an effective way for early diagnosis of AD.

Ideal AD biomarkers should be able to predict the incipient pathophysiological changes in AD brains and CSF, and can be simultaneously detected in peripheral body fluids such as blood. Also, high sensitivity and convenience for detection are necessary. As the brain tissues of AD patients are hard to obtain, it is limited to get enough information in AD brains. Therefore, in this study, we use GEO database to further

analyze the differentially expressed genes (DEGs) in AD brains, CSF and blood. We finally screened out a high-expressed DEG called *PTAFR* closely related to AD progression. Furthermore, its predictive efficacy and the possible mechanism involved in AD were also validated and investigated in APP/PS1 mice model and in LPS + Aβ-induced BV2 cells.

Materials And Methods

1. GEO Data Collection

We searched for "Alzheimer's disease" in GEO database (https://www.ncbi.nlm.nih.gov/geo/)，microarray datasets GSE1297 from the GPL96 platform, GSE63063 chip from the GPL10558 platform and the GSE110226 chip from the GPL10379 platform were downloaded. In GSE1297, according to the MMSE (Mini-mental State Examination, MMSE) score, hippocampal samples were divided into control group (MMSE>26, n=9), incipient AD group (MMSE: 20-26, n=7), moderated AD group (MMSE: 14-19, n=8), and severe AD group (MMSE<14, n=7). GSE63063 contained 135 control samples and 139 AD patients' blood samples, while GSE110226 included 6 samples of normal choroid plexus and 7 samples of choroid plexus from AD patients.

2. Conversion and difference analysis of raw data

The GEO2R interactive online tool (https://www.ncbi.nlm.nih.gov/geo/geo2r) was applied to convert the raw data into a recognizable format. The differential expression genes (DEGs) were identified with P <0.05 and |logFC|>1 as threshold values. The expression of genes obtained by VENN intersection was corrected by Bonferroni method.

3. GO and KEGG pathway enrichment analysis and protein interaction analysis

The online enrichment platform David (http://david-d.ncifcrf.gov/) was used to conduct enrichment analysis of KEGG pathway and GO function on DEGs and screen the top-10 significant biological pathways with P<0.05. Then, we used the bisoGenet plug-in in Cytoscape3.6.1 software to analyze the protein interaction of DEGs. Simultaneously, the protein interactions with the target gene *PTAFR* were evaluated through the String online tool (https://string-db.org/).

4. Brain samples and blood samples collection

C57BL/6 mice are sourced from the Experimental Animal Center of China Medical University, and APP/PS1 transgenic mice are from Jackson laboratory. All animal care and experimental procedures are in compliance with the "Ethical Standards for Animal Laboratory Animals" of China Medical University. We collected the hippocampus of 12-month-old APP/PS1 mice (n=5) and 12-month-old C57BL/6 mice (n=5). We chose to study only female mice because incidence of AD is biased towards female[9]. The right hemisphere was used for Western Blotting, while the left hemisphere was immersed in paraformaldehyde for immunofluorescence staining. Blood was obtained from the orbit. Then, the blood

samples were centrifuged at 3000 rpm for 10 minutes at room temperature. The bottom layer was collected and used for RNA extraction.

5. Cell Culture

The cells used in our experiment are BV2, SH-SY5Y, SVGp12. Mouse-derived microglial BV2 cells and human-derived neuroblastoma SH-SY5Y cells were purchased from the Institute of Basic Medicine Chinese Academy of Medical Sciences while human-derived astrocytes SVGp12 were purchased from Bei Na Chuang Lian company. Both BV2 and SVGp12 cells were cultured in DMEM medium, and SH-SY5Y cells were cultured in DMEM/F12 medium. All cells need to add 10% fetal bovine serum (FBS) and 100U/ml penicillin-streptomycin, and place them in a 37°C, 5% CO2 incubator for culture. We use cells of passage 5-20 for experiments.

6. Transfection and treatment of BV2 cells

We transfected the si-*PTAFR* plasmid (purchased from Shen Gong Bioengineering Co., Ltd.) into BV2 cells as required, and the transfection reagent was Lipofectamine 3000 (purchased from Thermo). In the nucleotide sequence of si-*PTAFR*, the sense strand is GCUAUGGGUCUUUGCUAACUUTT; the anti-sense strand is AAGUUAGCAAAGACCCAUAGCTT. When the cell density was about 60%-70%, cells were transfected by using Lipofectamine 3000 according to the manufacturer's instructions for 24 hours. 1μg/ml of LPS and 10μM/L of Aβ (Aβ25-35 were placed in a 37°C incubator for 7 days before use) were incubated for another 24h, then collected the corresponding proteins and mRNAs and stored them at -80°C.

7. Real-time PCR

We used the reverse transcription kit (Evo M-MLV RT Premix for qPCR) to reverse transcribe the extracted total RNA into complementary cDNA, and then conduct the qPCR kit (SYBR Green Premix Pro Taq HS qPCR Kit) according to the instructions required by the system (5μl SYBR, 0.2μl upstream and downstream primers, 0.2μl ROX, 1μl cDNA, 3.4μl DEPC water) for real-time quantitative PCR detection. The primers listed in this article are PTAFR, IL10, STAT3, and IL6. All primers were obtained from Sangon Biotech. The primer sequences are shown in Table 1. The results were processed by $2^{-\triangle\triangle CT}$ method to compare the relative expression of RNA.

Table1: Primer sequence list

Primer	Sequence (5'-3')
PTAFR-Forward	GAGTTTCGATACACGCTCTTTC
PTAFR-Reverse	CAAGTTAGCAAAGACCCATAGC
IL10-Forward	TTCTTTCAAACAAAGGACCAGC
IL10-Reverse	GCAACCCAAGTAACCCTTAAAG
STAT3-Forward	TGTCAGATCACATGGGCTAAAT
STAT3-Reverse	GGTCGATGATATTGTCTAGCCA
IL6-Forward	CTCCCAACAGACCTGTCTATAC
IL6-Reverse	CCATTGCACAACTCTTTTCTCA
GAPDH-Forward	AGCCTCGTCCCGTAGACAAAA
GAPDH-Reverse	TGGCAACAATCTCCACTTTGC

8. Western Blotting

The BV2 cells and brain tissue were homogenized with protein lysate containing protease inhibitors and the proteins were extracted, then quantified with a BCA kit (Bi Yun Tian company). Equal amounts of protein were separated by SDS-polyacrylamide gels and transferred to polyvinylidene fluoride membranes. Then, the membrane was incubated in a blocking solution (a mixture of TBST containing 0.1% Tween-20 and 5% BSA) for 1 h at room temperature, and placed in a primary antibody containing PTAFR(Abcam,1:200), IL10(Wanlei,1:1000), STAT3(CST,1:1000), IL6(Wanlei,1:1000), MAP2(CST,1:1000), and Syn (CST,1:1000) at 4°C overnight. The next day, after washing with TBST, the membrane was incubated with the corresponding HRP secondary antibody. The immune response band was observed by ECL with luminescence and quantified by measuring the density of each band using Image-J software.

9. CCK8 detection

The cell survival viability was assessed by CCK8 assay. First, SH-SY5Y cells were spread in a 96-well plate (n=5000 cells/well) and cultured for 24 hours. Then, the medium was changed to the transfected and modeled BV2 cell supernatant for 1h. 1μg/ml LPS and 10μM/L Aβ were given, and the culture was continued for 24h. After that, change the medium to serum-free DMEM medium containing 10% CCK8 reagent, 100μl per well, and incubate at 37°C for 2h. Finally, use a microplate reader to detect the absorbance at 450nm wavelength, and calculate the cell viability.

10. Flow cytometry to measure apoptosis

For apoptosis assays, SH-SY5Y cells were seeded in a 6-well plate (n=2*10^5 cells/well) and cultured for 24 hours. Then, the medium was changed to the transfected and modeled BV2 cell supernatant for 1h.

1μg/ml LPS and 10μM/L Aβ were given, and the culture was continued for 24h. Cells were washed twice with pre-cooled PBS, incubated with Annexin V-FITC and PI in the dark. Ultimately, cell apoptosis was analyzed by flow cytometer (BD Company).

11. Immunofluorescence

BV2 cells and SH-SY5Y cells were inoculated on a sterile cover glass into 12-well plates. After transfection and conditioned culture, the cells were fixed with 4% paraformaldehyde at room temperature. After washing with PBS, the cells were permeabilized with 0.5% TritonX-100 for 20 minutes. The cells and brain tissue were blocked with goat serum and stained with PTAFR or MAP2 in a humid box at 4°C overnight. Afterward, they were incubated with TRITC-conjugated rabbit anti-goat IgG for 1 h at 37°C in a dark and humid box, followed by counterstaining with DAPI. Finally, the immunofluorescence image was obtained by laser scanning of a confocal microscope.

12. MOE molecular docking

The protein secondary structure of PTAFR were downloaded from the PDB website (http://www1.rcsb.org/) while the three-dimensional structure of EGCG, donepezil, curcumin, memantine, and Huperzine A were acquired from the PubChem website (https://pubchem.ncbi.nlm.nih.gov/). Then, we imported the protein and small molecule drug structure into the MOE (2018 version) software and convert the protein secondary structure into the tertiary structure. At last, we perform molecular docking between protein and drugs after the small molecule drug is optimized.

13. Statistical Analysis

All data are statistically analyzed using GraphPad Prism 8.0.1 version. The data are expressed as mean ± standard deviation. Differences between groups were evaluated by one-way analysis of variance. All determinations were repeated three times. $P<0.05$ was considered statistically significant.

Results

32 DEGs was found closely related to AD progression by further analysis of GSE1297

To obtain the DEGs related to AD progression, we found GSE 1297 chip from GEO database. The GSE 1297 included the expression profiling of brain hippocampus from 22 postmortem samples of AD patients at various stages of severity (incipient, moderate, and severe AD). The DEGs were screened out with the criteria (|logFC|>1, $P< 0.05$), shown as Fig. 1a. There were 174 up-regulated DEGs and 54 down-regulated DEGs in incipient AD; 270 up-regulated DEGs and 157 down-regulated DEGs in moderate AD; 688 up-regulated DEGs and 367 down-regulated DEGs in severe AD (Fig. 1b). Then, VENN graph network tool (https://bioinfogp.cnb.csic.es/tools/venny/index.html) was employed to find the DEGs significantly changed in all the stages of AD, and 32 DEGs were obtained finally (Fig. 1c, Table 2). They were further

analyzed by heat map analysis by the Sangerbox program (Fig. 1d). It was shown that 25 genes were significantly up-regulated throughout the various stages of incipient, moderate and severe AD, including: *CR1, OGFOD3, AKAP13, MRPS12, ZDHHC17, ERF, UMOD, GRP107, PTGER4P2-CDK2AP2P2, HRP, RAD51B, NPAT, FGF20, RPL21P28, PTAFR, IL9R, AVPR2, LTB4R, PMS2P9, MYRF, SLC16A5, ATP11A, ITGB3, BGN, LOC389906*. And 6 genes such as *TNFRSF25, E2F5, BICD2, RFXAP, TAC1, B4GALT6* were significantly down-regulated in each stage of AD. Only *ITGB1* gene was up-regulated in incipient and moderate AD, while down-regulated in severe AD (Table.2). Therefore, considering for the characteristics of biomarkers, we focused on the 25 up-regulated DEGs in each stage of AD.

Table 2
DEGs in the brain hippocampus of incipient, moderate and severe AD in GSE1297

Gene name	Gene description	Incipient AD		Moderate AD		Severe AD	
		P-Val	logFC	P-Val	logFC	P-Val	logFC
CR1	Complement component 3b/4b receptor 1 (Knops blood group)	0.042	1.04	0.006	1.62	0.028	1.10
OGFOD3	2-oxoglutarate and iron dependent oxygenase domain containing 3	0.038	1.06	0.007	1.02	0.003	1.46
AKAP13	A- kinase anchoring protein 13	0.031	1.11	0.035	1.08	0.001	1.29
MRPS12	Mitochondrial ribosomal protein S12	0.038	1.11	0.010	1.40	0.005	1.72
ZDHHC17	Zinc finger DHHC-type containing 17	0.017	1.15	0.001	1.44	0.007	1.03
ERF	ETS2 repressor factor	0.003	1.18	0.001	1.44	0.001	1.38
UMOD	Uromodulin	0.024	1.20	0.026	1.09	0.013	1.16
ITGB1	Integrin subunit beta 1	0.038	1.25	0.044	1.38	0.001	-1.39
GPR107	G protein-coupled receptor 107	0.021	1.26	0.018	1.46	0.029	1.21
PTGER4P2-CDK2AP2P2	PTGER4P2-CDK2AP2P2 readthrough, transcribed pseudogene	0.001	1.32	0.001	1.48	0.003	1.40
HPR	Haptoglobin-related protein	0.025	1.32	0.033	1.22	0.002	1.77
RAD51B	RAD51 paralog B	0.005	1.33	0.016	1.21	0.005	1.23
NPAT	Nuclear protein, coactivator of histone transcription	0.002	1.37	0.012	1.11	0.004	1.35
FGF20	Fibroblast growth factor 20	0.002	1.48	0.006	1.32	0.016	1.44
RPL21P28	Ribosomal protein L21 pseudogene 28	0.017	1.52	0.008	1.41	0.022	1.53
PTAFR	Platelet activating factor receptor	0.007	1.53	0.000	1.90	0.000	2.35
IL9R	Interleukin 9 receptor	0.003	1.53	0.009	1.09	0.000	1.98
AVPR2	Arginine vasopressin receptor 2	0.003	1.55	0.001	1.64	0.005	1.74

Gene name	Gene description	Incipient AD		Moderate AD		Severe AD	
		P-Val	logFC	P-Val	logFC	P-Val	logFC
LTB4R	Leukotriene B4 receptor	0.000	1.58	0.003	1.29	0.001	1.76
PMS2P9	PMS1 homolog 2, mismatch repair system component pseudogene 9	0.006	1.64	0.002	1.60	0.023	1.16
MYRF	Myelin regulatory factor	0.018	1.66	0.002	1.43	0.001	1.53
SLC16A5	Solute carrier family 16member 5	0.010	1.67	0.014	1.47	0.008	1.65
ATP11A	ATPase phospholipid transporting 11A	0.000	1.68	0.000	1.85	0.002	1.50
ITGB3	Integrin subunit beta 3	0.006	1.86	0.010	1.86	0.018	2.02
BGN	Biglycan	0.002	1.96	0.016	1.47	0.020	1.59
LOC389906	Zinc finger protein 839 pseudogene	0.000	2.66	0.005	1.70	0.000	2.64
TNFRSF25	TNF receptor superfamily member 25	0.027	-1.11	0.019	-1.13	0.044	-1.30
E2F5	E2F transcription factor 5	0.023	-1.35	0.005	-1.53	0.027	-1.29
BICD2	BICD cargo adaptor 2	0.020	-1.16	0.011	-1.21	0.004	-1.86
RFXAP	Regulatory factor X associated protein	0.018	-1.13	0.004	-1.49	0.012	-1.15
TAC1	Tachykinin precursor 1	0.021	-1.08	0.007	-1.39	0.011	-1.50
B4GALT6	Beta-1,4-galactosyltransferase 6	0.032	-1.06	0.002	-1.46	0.002	-1.41

In order to identify the dominant pathways of the screening DEGs and their biological roles, we performed enrichment analysis of the KEGG pathway and GO function by David network enrichment tool (http://david-d.ncifcrf.gov/) and obtained top-10 biological pathways with statistical significance (Fig. 2a). The biological processions were hematopoietic cell lineage, viral entry into host cells, mesodermal cell differentiation, inflammatory response, cell adhesion mediated by integrin, cell-substrate adhesion, heterotypic cell-cell adhesion, positive regulation of cell proliferation, extracellular matrix organization and leukocyte cell-cell adhesion. Afterwards, we also explored the interactions between the 32 DEGs using the bisoGenet plug-in of Cytoscape3.6.1 software. It was found that 22 genes had the possible interactions with core pathogenic genes APP of AD, such as *PTAFR, BGN, E2F5, BICD2, SLC16A5,*

AVPR2, TNFRSF25, IL9R, RFXAP, AKAP13, CR1, NPAT, RAD51B, GPR107, ITGB1, ITGB3, ERF, MRPS12, TAC1, OGFOD3, LTB4R, and *ZDHHC17* (Fig. 2b).

Up-regulated PTAFR in peripheral blood, cerebrospinal fluid and hippocampus of AD patients

As we obtained 32 DEGs in the hippocampus of AD patients in different stages, it was considered for the possible application as potential biomarkers for AD diagnosis. The potential biomarkers should significantly change with the occurrence and progression of AD, it is essential the changes of DEGs in hippocampus synchronize with the changes in blood and cerebrospinal fluid (CSF). Therefore, we found out the CSF chip (GSE110226) and the blood chip (GSE63063) for the further investigation. VENN graph network tool was used for screening the target DEGs changed in blood, CSF and hippocampus of AD. We finally got two DEGs, *PTAFR* and *AKAP13* (Fig. 3a). Then, the possible correlations between the mRNA expressions of *PTAFR* and *AKAP13* with MMSE scores were examined. We found that the mRNA expression of *PTAFR* was correlated with the MMSE score ($P = 0.0006$), while that of AKAP13 was not significantly correlated with MMSE score ($P = 0.1308$), shown in Fig. 3b. Also, the Braak staging was more strongly correlated with *PTAFR* than that with AKAP13 (*PTAFR*, $P < 0.0001$; AKAP13, $P = 0.0274$; Fig. 3c). We also found the expression of *PTAFR* was positively correlated with neurofibrillary tangles scores than AKAP13(*PTAFR*, $P = 0.0015$; AKAP13, $P = 0.1078$; Fig. 3d). The mRNA expression of *PTAFR* was also gradually increased with AD progression from incipient to severe AD ($P < 0.05$, Fig. 3e*)*, while AKAP13 did not follow this manner (Fig.S1a). Besides, both PTAFR and AKAP3 were all increased in both choroid plexus and peripheral blood (Fig. 3f & Fig.S1a). *PTAFR* was also highly expressed in entohinal cortex, hippocampus, and temporal cortex in AD brains, while *AKAP13* was just highly expressed in hippocampus (Fig. 3h & Fig.S1c). Furthermore, we investigated the possible mechanism of PTAFR involved in AD progression. Using the AlzData online network platform (http://www.alzdata.org)[10], the PTAFR is only highly expressed in microglia which contributes with inflammatory response in the pathogenesis of AD while AKAP13 is expressed in many cell lines (Fig. 3g, S1b). Taken together, our findings suggested that *PTAFR* might be the target biomarkers with higher efficacy for AD diagnosis.

Further validation for the highly-expressed PTAFR in 12-month-old APP/PS1 mice, and in BV2 cells

Our previous results of GEO database indicated PTAFR was a possibly potential biomarker highly expressed in AD patients, so next we validated it both in vivo and in vitro. We performed the validation on a 12-month-old APP/PS1 double transgenic AD mouse model. As we expected, it was showed that the PTAFR in APP/PS1 mice was significantly increased in both mRNA and protein levels ($P < 0.01$, Fig. 4a, b, c), compared with the age-matched C57 BL/6J mice. The peripheral blood levels of PTAFR in APP/PS1 mice was also significantly increased ($P < 0.01$, Fig. 4a).

Also, we validated the results in vitro. As we previously mentioned, the predictive results on AlzData platform showed PTAFR was specifically highly expressed in microglia compared with other neural cell in central nervous system. A homologous sequence alignment of murine and human PTAFR gene were performed, and it was indicated the PTAFR gene of murine and homo sapiens are in high homology (Fig. S2c). Therefore, we examined the PTAFR mRNA and protein levels in different neural cell such as BV2 (microglia-like), SH-SY5Y(neuron-like), and SVGp12 (astrocyte-like) cell lines. We found that after LPS + Aβ treatment, the mRNA and protein levels of PTAFR is significantly elevated in BV2 cells ($P < 0.01$, Fig. 4a, b, d), while there were no significant changes of SVGp12 or SH-SY5Y cells compared with control group ($P > 0.05$, Fig. S2a, b), indicating that PTAFR was high-expressed gene in microglia.

By literature reviewing, *PTAFR* is closely related to the secretion of inflammatory factors in kidney injury and retinal neovascularization[11–13], indicating neuroinflammation mediated by microglia might be the possible mechanism of PTAFR involved in AD progression. First, we found that PTAFR is closely associated with the inflammatory factors IL-10 and STAT3 by the STRING online tool (https://string-db.org/) (Fig. 5a). Extensive studies revealed that the IL10-STAT3 pathway was involved in the occurrence of many diseases [14–19]. Then, we hypothesized PTAFR kindled the microglia-mediated neuroinflammation via IL10-STAT3 signaling and exaggerated the microenvironment of neurons in the procession of AD. After LPS and Aβ treatment, the mRNA and protein levels of IL-10 were decreased, and those of STAT3 and IL-6 were elevated, following the PTAFR up-regulation ($P < 0.05$, Fig. 5b-d). Further, we silenced PTAFR gene in BV2 cells, and found that the mRNA and protein levels of IL-10 were increased, while those of STAT3 and IL-6 were decreased ($P < 0.05$, Fig. 5b-d).

Then, the conditional medium (CM) of the treated BV2 cells was given to SH-SY5Y cells treated with LPS + Aβ to investigate the subsequent inflammatory efficacy of microglia on neurons. The CM of LPS + Aβ-induced BV2 cells significantly reduced the cell viability of SH-SY5Y cells ($P < 0.0001$, Fig. 5e-f), while the CM of LPS + Aβ-induced BV2 cells after silencing PTAFR improved the cell viability of SH-SY5Y cells in both CCK8 experiment and Annexin V/PI flow cytometry ($P < 0.001$, Fig. 5e-f). Besides, the CM also remarkedly enhanced the expression of neuroplasticity indexes MAP2 and Syn (Fig. 5g, h). Taken together, PTAFR, as a potential biomarker, exaggerated microglia-mediated microenvironment by increasing the inflammatory factors via IL10-STAT3 signaling.

Targeted docking of PTAFR with anti-AD drugs commonly used in clinical practice

As we mentioned previously, PTAFR was verified to play an important role in exaggerating the microglia-mediated neuronal microenvironment by IL10-STAT3 signaling, and closely correlated with AD progression. That is to say, it could be considered as a potential biomarker or an essential point for R&D of anti-AD drugs. Here, we made targeted molecular docking of PTAFR with several drugs recognized in clinical and scientific research for AD treatment, such as donepezil, memantine, EGCG, curcumin, and Huperzine A. The molecular docking was performed by MOE software. S value obtained after docking is used for evaluation of the possible binding. If S<-7 it is considered to have the probability of binding with

each other. EGCG is considered as a potential compound with anti-AD efficacy, the docking result showed it could possibly be bound with PTAFR (S=-7.7826, Fig. 6a). Donepezil is a medication used to treat mild or moderated AD, and commonly used in clinical practice. We also found the possible bind sites (S=-7.5199, Fig. 6b). Curcumin, another compound found to have neuroprotective efficacy, can bind with PTAFR, which S=-7.5698 (Fig. 6c). However, the S values of memantine and Huperzine A were − 5.3495 and S=-5.3781, respectively (Fig. 6d, e). It was also indicated that those compounds with planar structure with multiple benzene ring such as EGCG, curcumin, and donepezil seemed to be more likely to bind with PTAFR, while those compounds with stereo conformation, such as memantine and huperzine A, have significantly decreased binding effects on PTAFR. These results indicated that PTAFR could be combined with some anti-AD drugs, and might be used as a potential target for the treatment of AD in the future.

Discussion

The pathophysiological changes of AD often precede the major clinical symptoms such as cognitive dysfunction, as well as the characteristic pathological changes such as Aβ deposition and Tau hyperphosphorylation [20]. Therefore, early diagnosis of AD and the intervention targeting initial events of AD will benefit the prognosis and effectively improve the quality of life. At present, AD diagnosis mainly relies on MMSE score, ^{18}FDG-PET, CT or MRI, and the identification of T-tau, p-tau, Aβ42 and other biomarkers in cerebrospinal fluid [7, 21, 22]. However, they still have shortcomings such as high cost, lack of specificity, or invasive detection. Therefore, it is of great significance to find candidate biomarkers for early diagnosis of AD and to develop intervention strategies for early diagnosis and treatment of AD. Here, we discovered a potential biomarker named PTAFR screening out of GEO database and validated its efficacy in vivo and in vitro.

The ideal AD biomarker should be able to warn early AD brain lesions, detect in peripheral body fluids, have correlation with brain lesions, and be sensitive and simple in detection. Human brain tissue is extremely difficult to obtain and the related ethics are limited, so we screened the potential candidates in GEO database. 32 DEGs related to the progress of AD were got by GSE1297, they also closely related to inflammation processes, and 22 of them interacted with the core disease-causing gene APP of AD. Castillo et al found that the expression of genes closely related to inflammatory response were significantly increased in $APP^{NL-GF/NL-GF}$ mice[23]. Venegas et al found that the activation of inflammasomes is closely related to the formation and progression of Aβ plaques in AD[24]. Welikovitch's study proved that the neuron-specific inflammatory response may be earlier than the formation of Aβ plaques[25]. These above studies suggested that there was a close correlation between the inflammatory response and Aβ deposition in the end-stage AD, which also supported our results. To find ideal biomarkers reflecting the same changes in peripheral fluids as in the brain tissues, we further found a peripheral blood chip GSE63063 and the choroid plexus chip GSE110226. PTAFR was finally found to correlate with the severity of AD MMSE score, Braak staging and neurofibrillary tangle scores synchronously. However, there is no report related to PTAFR to reveal the predictive role in AD. Therefore, PTAFR gene became the focus of our follow-up research. We performed verification on 12-month-old

APP/PS1 mice and found that PTAFR was highly expressed in the brain and peripheral blood of APP/PS1 mice, which was consistent with the predicted results, suggesting that PTAFR had the potential to be a possibly candidate biomarker for AD diagnosis.

As a platelet activating factor receptor, PTAFR plays an important role in many diseases. It has been reported in the literature that the expression of PTAFR in breast cancer cells and osteoclasts was significantly increased, and when PTAFR expression was down-regulated, the breast cancer cell migration and osteoclast production were prevented in breast cancer bone metastasis models[26]. Besides, PTAFR down-regulation was also corelated to the proliferation of cardiac fibroblasts and the deposition of collagen, finally inhibiting the fibrous fibers after myocardial infarction in cardiac fibroblasts treated with angiotensin II [27]. However, PTAFR is rarely involved in the neurological field, and the role and pathogenic mechanism in AD have not been reported. Specially, PTAFR was highly expressed in microglia, while no increased expression was found in astrocytes, oligodendrocytes, or neurons by AlzData website. Further, we also found PTAFR had the specific high-expression in BV2 cells. So, we illustrated that the function of PTAFR gene in central nervous system correlated with microglia-mediate biological process. Microglia contributes to the neuroinflammation and mediates the microenvironment of neurons. Previous studies also found that PTAFR distributed on the surface of vascular endothelial cells could increase IL-1β expression, leading to inflammatory-dependent vascular occlusion in the ischemic retinopathy model [13]. In kidney injury model, PTAFR is highly expressed, and further aggravated the kidney injury by inducing the expression of the inflammatory factor TNFα[12]. Besides, in the renal fibrosis model induced by a large amount of ethanol intake, the expression of the inflammatory factor TGFβ and closely related indicators of renal fibrosis were significantly decreased in the PTAFR knockout mice, and the renal fibrosis was inhibited[11]. Furthermore, we also found that the expression of PTAFR was significantly increased in BV2 cells induced by LPS + Aβ, suggesting that PTAFR might be involved in the microglia-mediated inflammation of AD. However, almost no studies were reported about the possible mechanism of PTAFR in AD. We analyzed the possible interacting proteins with PTAFR by STRING online tool, and found IL10-STAT3 might closely related with PTAFR. Our study revealed IL-10 was increased, and STAT3 and IL-6 were increased after silencing PTAFR in BV2 cells. After conditioned culture of SH-SH5Y cells with treated BV2 cells, the survival and plasticity of SH-SH5Y cells were enhanced after PTAFR silence, suggesting PTAFR promoted the microglia-mediated neuroinflammation through IL10-STAT3 signaling and exaggerated the neuronal microenvironment in AD. IL-10 and STAT3 is involved in the occurrence and development of many diseases, such as Alzheimer's disease, breast cancer, glioma, autosomal dominant hereditary high IgE syndrome and so on[28–31]. Kiyota’s research found that IL-10 significantly reduced neuroinflammation, enhanced neuron generation, and improved spatial cognitive impairment in APP/PS1 mice[32]. Reichenbach's research confirmed that APP/PS1 transgenic mice with STAT3 knockout reduced Aβ plaque deposition in the brain, inhibited astrocyte proliferation and secretion of pro-inflammatory factors, and improved learning and memory impairment[33]. The above studies suggested that IL-10 and STAT3 were involved in the AD inflammatory response, supporting our findings. Therefore, it is the first report to reveal the relationship between PTAFR and IL10-STAT3 signaling in AD.

Since PTAFR was confirmed to be used as a potential biomarker for AD diagnosis, and as a possible target closely related to inflammation, can it be used as a potential target for drug therapy, or as a target to develop new anti-AD drugs? For the first time, we conducted MOE molecular docking between PTAFR and several drugs or compounds that are recognized in clinical and scientific research for the treatment of AD, and we found that PTAFR and these anti-AD drugs had a certain degree of combination. Among them, PTAFR has the highest binding degree with EGCG, donepezil and curcumin, indicating that the treatment of EGCG, donepezil or curcumin could interact with PTAFR to a certain extent, thereby exerting anti-inflammatory effects in AD. The above results further highlighted the potential significance of PTAFR as an AD biomarker and therapeutic target, and provided a possible reference for the molecular design of new anti-AD drugs.

In summary, PTAFR was a potential biomarker for early AD diagnosis and treatment correlated with microglia-mediated microenvironment, and an important possible target to make novel strategy for clinical treatment and new drug discovery in AD.

Conclusions

As a gene that is highly expressed in AD brain tissue, peripheral blood and cerebrospinal fluid, PTAFR were found to be a potential candidate biomarker for AD diagnosis. And PTAFR was highly-expressed in microglia, and induced the neuron inflammatory response to exaggerate the microenvironment of AD neurons via IL10-STAT3 signaling in vivo and in vitro. It also provided us a novel intervention target for AD treatment, and a possible reference for the molecular design of new anti-AD drugs.

Declarations

Data Availability

The datasets during and/or analyzed during the current study are available from the corresponding author on reasonable request.

Acknowledgments

The authors would like to acknowledge the Key Laboratory of Precision Diagnosis and Treatment of Gastrointestinal Tumors, Ministry of Education (China Medical University, Shenyang, China) and Liaoning Medical Diagnosis and Treatment Center (Liaoning Province, China) for providing the space and equipment for conducting the experiments.

Funding

This work was supported by grants from Key R&D Plan Guidance Project of Liaoning Province (2018225089), the National Natural Science Foundation of China (81901309, 81603112), Doctoral Research Startup Fund Project of Liaoning Province (2019-BS-289), Key R&D Project of Liaoning

Provincial Department of Science and Technology (ZF2019037), General Project of Liaoning Provincial Department of Science and Technology (2020-MS-161).

Author contributions

J.L. and M.L. designed and conceived the research. J.L. and S.L. performed the cell experiments. J.L., T.M. and M.X. conducted the animal experiments. J.L. and M.L. collected and analyzed the data. J.L., M.L. wrote and revised the manuscript. C.L., X.Z., W.Y., K.D., Y.W., J.T., W.J., Y.W. and X.W. directed the article. All authors approved the final manuscript.

Ethics declarations

All animal care and experimental procedures were in line with the Laboratory Animal Ethical Standards of China Medical University (201907127) as well as the Standard Medical Laboratory Animal's Care and Use Protocols.

Conflict of interest

The authors have declared no conflict of interest.

Code Availability

Not applicable.

Consent to participate

Not applicable.

Consent to Publication

Not applicable.

References

1. *2020 Alzheimer's disease facts and figures.* Alzheimers Dement, 2020.
2. Robinson, M., B.Y. Lee, and F.T. Hane, *Recent Progress in Alzheimer's Disease Research, Part 2: Genetics and Epidemiology.* J Alzheimers Dis, 2017. **57**(2): p. 317–330.
3. McKhann, G.M., D.S. Knopman, H. Chertkow, et al., *The diagnosis of dementia due to Alzheimer's disease: recommendations from the National Institute on Aging-Alzheimer's Association workgroups on diagnostic guidelines for Alzheimer's disease.* Alzheimers Dement, 2011. **7**(3): p. 263-9.
4. Kerbler, G.M., J. Fripp, C.C. Rowe, et al., *Basal forebrain atrophy correlates with amyloid beta burden in Alzheimer's disease.* Neuroimage Clin, 2015. **7**: p. 105 – 13.

5. Hyman, B.T., C.H. Phelps, T.G. Beach, et al., *National Institute on Aging-Alzheimer's Association guidelines for the neuropathologic assessment of Alzheimer's disease.* Alzheimers Dement, 2012. **8**(1): p. 1–13.
6. Sperling, R.A., P.S. Aisen, L.A. Beckett, et al., *Toward defining the preclinical stages of Alzheimer's disease: recommendations from the National Institute on Aging-Alzheimer's Association workgroups on diagnostic guidelines for Alzheimer's disease.* Alzheimers Dement, 2011. **7**(3): p. 280 – 92.
7. Hane, F.T., M. Robinson, B.Y. Lee, et al., *Recent Progress in Alzheimer's Disease Research, Part 3: Diagnosis and Treatment.* J Alzheimers Dis, 2017. **57**(3): p. 645–665.
8. Ma, G., M. Liu, K. Du, et al., *Differential Expression of mRNAs in the Brain Tissues of Patients with Alzheimer's Disease Based on GEO Expression Profile and Its Clinical Significance.* Biomed Res Int, 2019. **2019**: p. 8179145.
9. Jiao, S.S., X.L. Bu, Y.H. Liu, et al., *Sex Dimorphism Profile of Alzheimer's Disease-Type Pathologies in an APP/PS1 Mouse Model.* Neurotox Res, 2016. **29**(2): p. 256 – 66.
10. Xu, M., D.F. Zhang, R. Luo, et al., *A systematic integrated analysis of brain expression profiles reveals YAP1 and other prioritized hub genes as important upstream regulators in Alzheimer's disease.* Alzheimers Dement, 2018. **14**(2): p. 215–229.
11. Latchoumycandane, C., M. Hanouneh, L.E. Nagy, et al., *Inflammatory PAF Receptor Signaling Initiates Hedgehog Signaling and Kidney Fibrogenesis During Ethanol Consumption.* PLoS One, 2015. **10**(12): p. e0145691.
12. Latchoumycandane, C., L.E. Nagy, and T.M. McIntyre, *Myeloperoxidase formation of PAF receptor ligands induces PAF receptor-dependent kidney injury during ethanol consumption.* Free Radic Biol Med, 2015. **86**: p. 179 – 90.
13. Bhosle, V.K., J.C. Rivera, T.E. Zhou, et al., *Nuclear localization of platelet-activating factor receptor controls retinal neovascularization.* Cell Discov, 2016. **2**: p. 16017.
14. Degboe, Y., B. Rauwel, M. Baron, et al., *Polarization of Rheumatoid Macrophages by TNF Targeting Through an IL-10/STAT3 Mechanism.* Front Immunol, 2019. **10**: p. 3.
15. Cevey, A.C., F.N. Penas, C.D. Alba Soto, et al., *IL-10/STAT3/SOCS3 Axis Is Involved in the Anti-inflammatory Effect of Benznidazole.* Front Immunol, 2019. **10**: p. 1267.
16. Campana, L., P.J. Starkey Lewis, A. Pellicoro, et al., *The STAT3-IL-10-IL-6 Pathway Is a Novel Regulator of Macrophage Efferocytosis and Phenotypic Conversion in Sterile Liver Injury.* J Immunol, 2018. **200**(3): p. 1169–1187.
17. Zhang, X., Y. Zeng, Q. Qu, et al., *PD-L1 induced by IFN-gamma from tumor-associated macrophages via the JAK/STAT3 and PI3K/AKT signaling pathways promoted progression of lung cancer.* Int J Clin Oncol, 2017. **22**(6): p. 1026–1033.
18. Shirakawa, K., J. Endo, M. Kataoka, et al., *IL (Interleukin)-10-STAT3-Galectin-3 Axis Is Essential for Osteopontin-Producing Reparative Macrophage Polarization After Myocardial Infarction.* Circulation, 2018. **138**(18): p. 2021–2035.

19. Wang, G., B. Xu, F. Shi, et al., *Protective Effect of Methane-Rich Saline on Acetic Acid-Induced Ulcerative Colitis via Blocking the TLR4/NF-kappaB/MAPK Pathway and Promoting IL-10/JAK1/STAT3-Mediated Anti-inflammatory Response.* Oxid Med Cell Longev, 2019. **2019**: p. 7850324.
20. Tan, C.C., J.T. Yu, and L. Tan, *Biomarkers for preclinical Alzheimer's disease.* J Alzheimers Dis, 2014. **42**(4): p. 1051-69.
21. Wolinsky, D., K. Drake, and J. Bostwick, *Diagnosis and Management of Neuropsychiatric Symptoms in Alzheimer's Disease.* Curr Psychiatry Rep, 2018. **20**(12): p. 117.
22. Guest, F.L., H. Rahmoune, and P.C. Guest, *Early Diagnosis and Targeted Treatment Strategy for Improved Therapeutic Outcomes in Alzheimer's Disease.* Adv Exp Med Biol, 2020. **1260**: p. 175–191.
23. Castillo, E., J. Leon, G. Mazzei, et al., *Comparative profiling of cortical gene expression in Alzheimer's disease patients and mouse models demonstrates a link between amyloidosis and neuroinflammation.* Sci Rep, 2017. **7**(1): p. 17762.
24. Venegas, C., S. Kumar, B.S. Franklin, et al., *Microglia-derived ASC specks cross-seed amyloid-beta in Alzheimer's disease.* Nature, 2017. **552**(7685): p. 355–361.
25. Welikovitch, L.A., S. Do Carmo, Z. Magloczky, et al., *Early intraneuronal amyloid triggers neuron-derived inflammatory signaling in APP transgenic rats and human brain.* Proc Natl Acad Sci U S A, 2020. **117**(12): p. 6844–6854.
26. Hou, T., Y. Lou, S. Li, et al., *Kadsurenone is a useful and promising treatment strategy for breast cancer bone metastases by blocking the PAF/PTAFR signaling pathway.* Oncol Lett, 2018. **16**(2): p. 2255–2262.
27. Zhao, X.S., Y. Ren, Y. Wu, et al., *MiR-30b-5p and miR-22-3p restrain the fibrogenesis of post-myocardial infarction in mice via targeting PTAFR.* Eur Rev Med Pharmacol Sci, 2020. **24**(7): p. 3993–4004.
28. Porro, C., A. Cianciulli, T. Trotta, et al., *Curcumin Regulates Anti-Inflammatory Responses by JAK/STAT/SOCS Signaling Pathway in BV-2 Microglial Cells.* Biology (Basel), 2019. **8**(3).
29. Chen, L., Y. Shi, X. Zhu, et al., *IL10 secreted by cancerassociated macrophages regulates proliferation and invasion in gastric cancer cells via cMet/STAT3 signaling.* Oncol Rep, 2019. **42**(2): p. 595–604.
30. Yao, Y., H. Ye, Z. Qi, et al., *B7-H4(B7x)-Mediated Cross-talk between Glioma-Initiating Cells and Macrophages via the IL6/JAK/STAT3 Pathway Lead to Poor Prognosis in Glioma Patients.* Clin Cancer Res, 2016. **22**(11): p. 2778–2790.
31. Paulson, M.L., A.F. Freeman, and S.M. Holland, *Hyper IgE syndrome: an update on clinical aspects and the role of signal transducer and activator of transcription 3.* Curr Opin Allergy Clin Immunol, 2008. **8**(6): p. 527 – 33.
32. Kiyota, T., K.L. Ingraham, R.J. Swan, et al., *AAV serotype 2/1-mediated gene delivery of anti-inflammatory interleukin-10 enhances neurogenesis and cognitive function in APP + PS1 mice.* Gene Ther, 2012. **19**(7): p. 724 – 33.

33. Reichenbach, N., A. Delekate, M. Plescher, et al., *Inhibition of Stat3-mediated astrogliosis ameliorates pathology in an Alzheimer's disease model.* EMBO Mol Med, 2019. **11**(2).

Figures

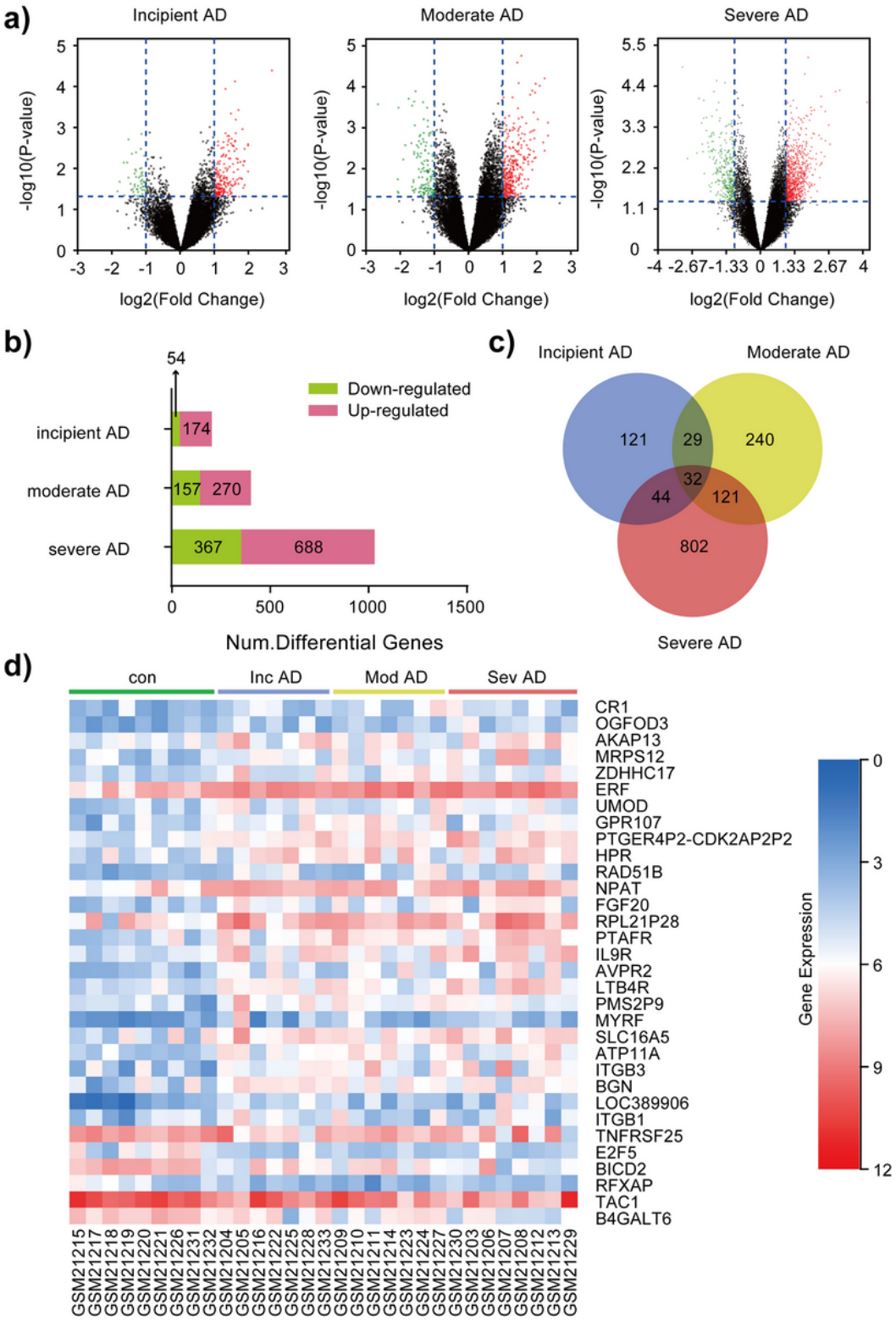

Figure 1

DEGs were screened out from the hippocampus of AD patients with GSE1297. GSE 1297 included the expression profiling of hippocampal CA1 tissues from 22 AD postmortem samples at various stages of severity. 7, 8, and 7 subjects diagnosed with incipient, moderate, and severe AD respectively. The DEGs were screened out with the criteria (|logFC|>1, P<0.05) (a) Volcano maps of DEGs in the incipient, moderate, and severe AD. (b) The distribution of up-regulated and down-regulated of DEGs in each stage. (c) 32 DEGs were screened out of the intersection of different AD stages by VENN map. (d) Heat map distribution of 32 DEGs.

a)

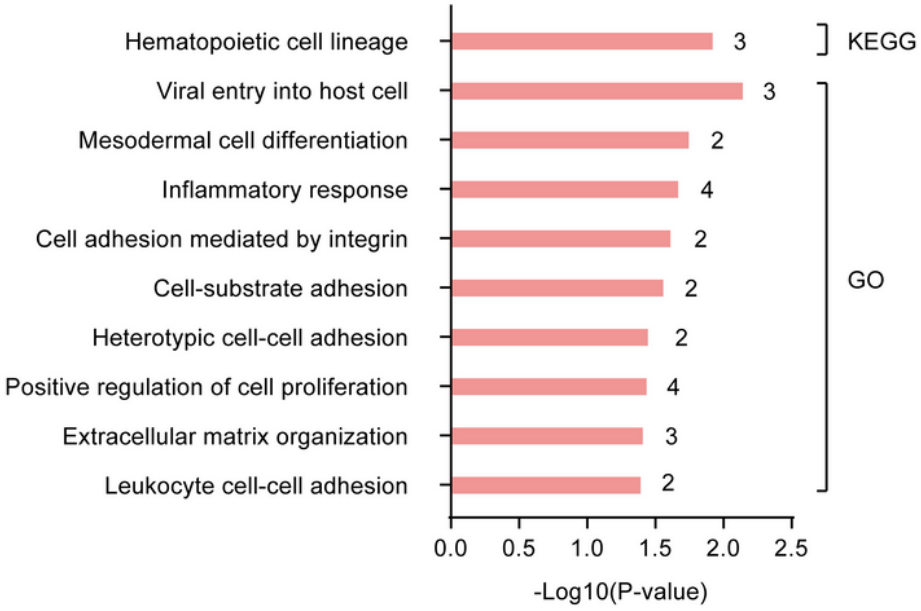

b)

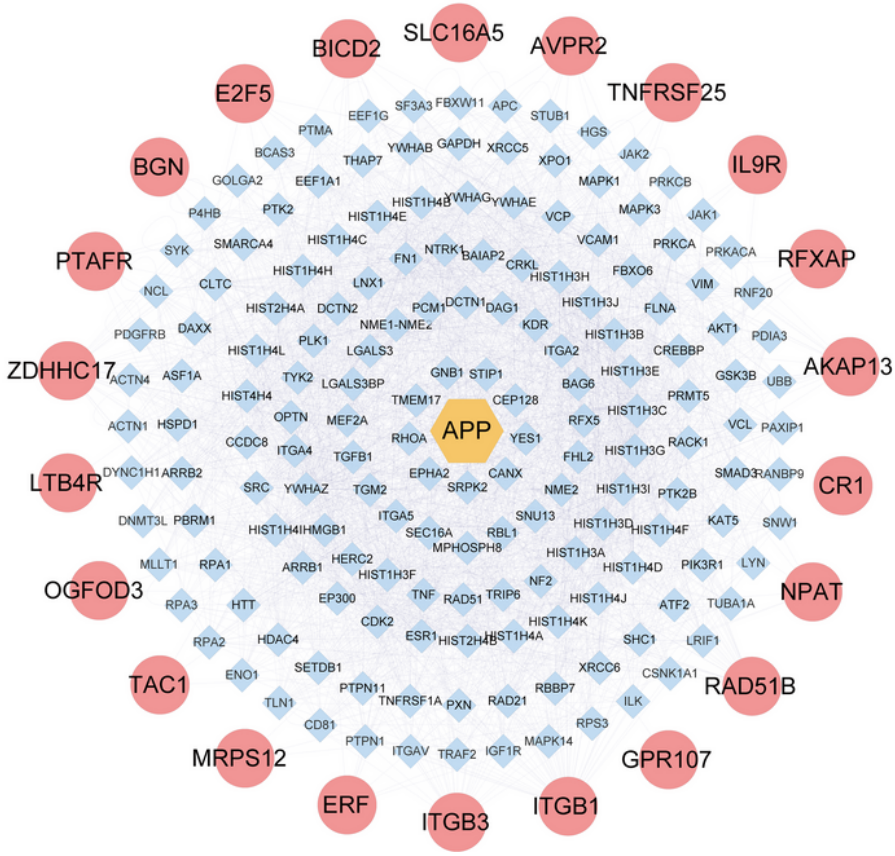

Figure 2

Enrichment and PPI network analysis of DEGs in the hippocampus of AD patients in GSE1297. (a) The top-10 biological processes with statistical significance enriched by KEGG pathway and Go function from 32 DEGs. (b) Protein interaction relationship between the pathogenic genes APP and the 32 DEGs using bisoGenet plug-in of Cytoscape3.6.1 software.

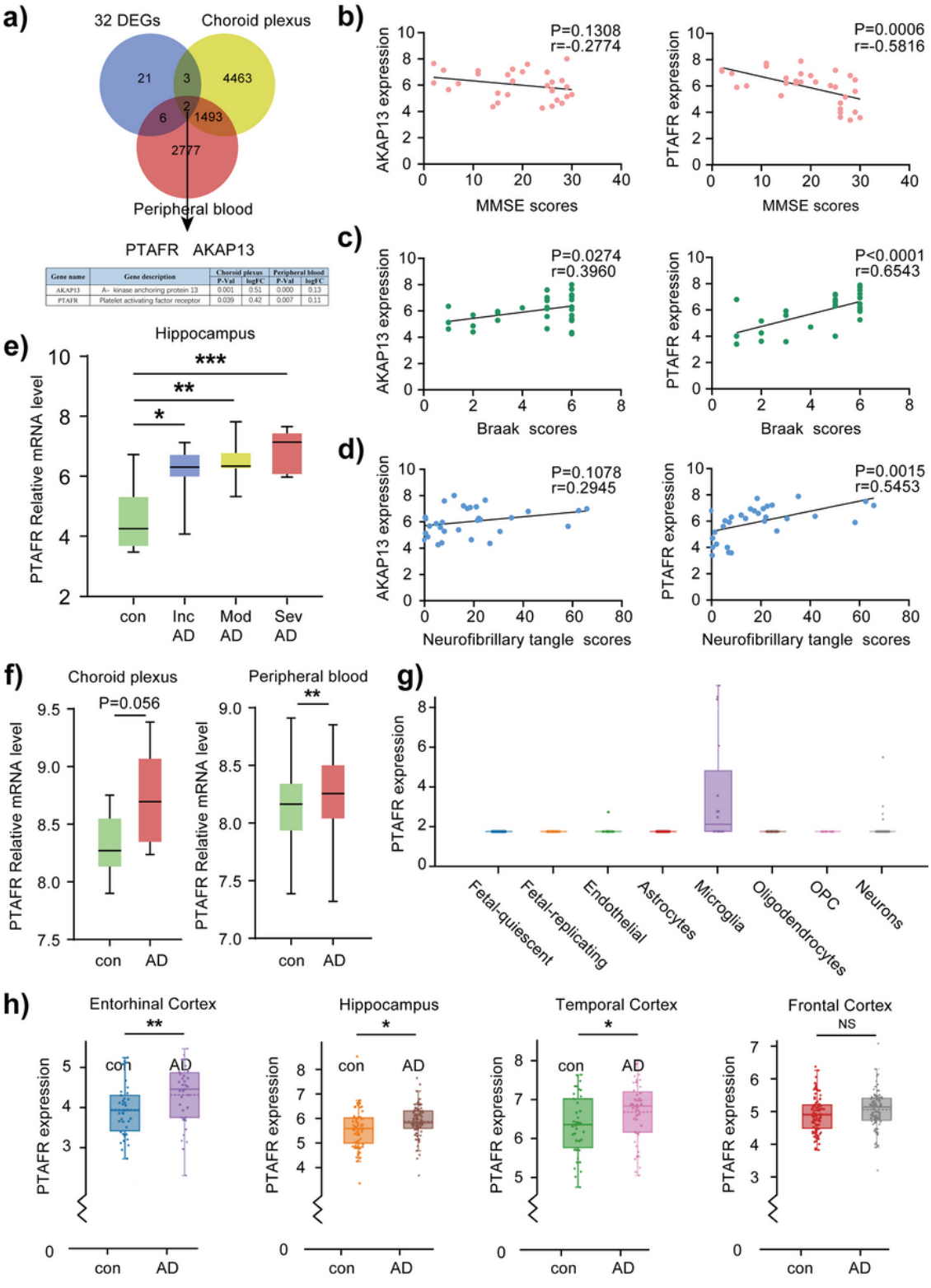

Figure 3

PTAFR was specifically and highly expressed in the peripheral blood, cerebrospinal fluid and hippocampus of AD patients. (a) The analysis of DEGs in the hippocampus, CSF, and peripheral blood of AD patients by VENN map. (b) The correlations between the mRNA expressions of AKAP13 (left) or PTAFR (right) and MMSE scores by Linear regression. (c) The correlations between the mRNA expressions of AKAP13 (left) or PTAFR (right) and Braak scores by Linear regression. (d) The correlations between the mRNA expressions of AKAP13 (left) or PTAFR (right) and neurofibrillary tangles scores by Linear regression. (e) The mRNA expression of PTAFR in AD hippocampus throughout the AD progression. (f) PTAFR gene mRNA expression in AD cerebrospinal fluid and peripheral blood. (g) PTAFR expression in different types of neural cells in the AlzData platform. (h) The mRNA expression levels of PTAFR in the entorhinal cortex, hippocampus, temporal cortex and frontal cortex, respectively. *P<0.05, **P<0.01, ***P<0.001, ****P<0.001, compared with control group.

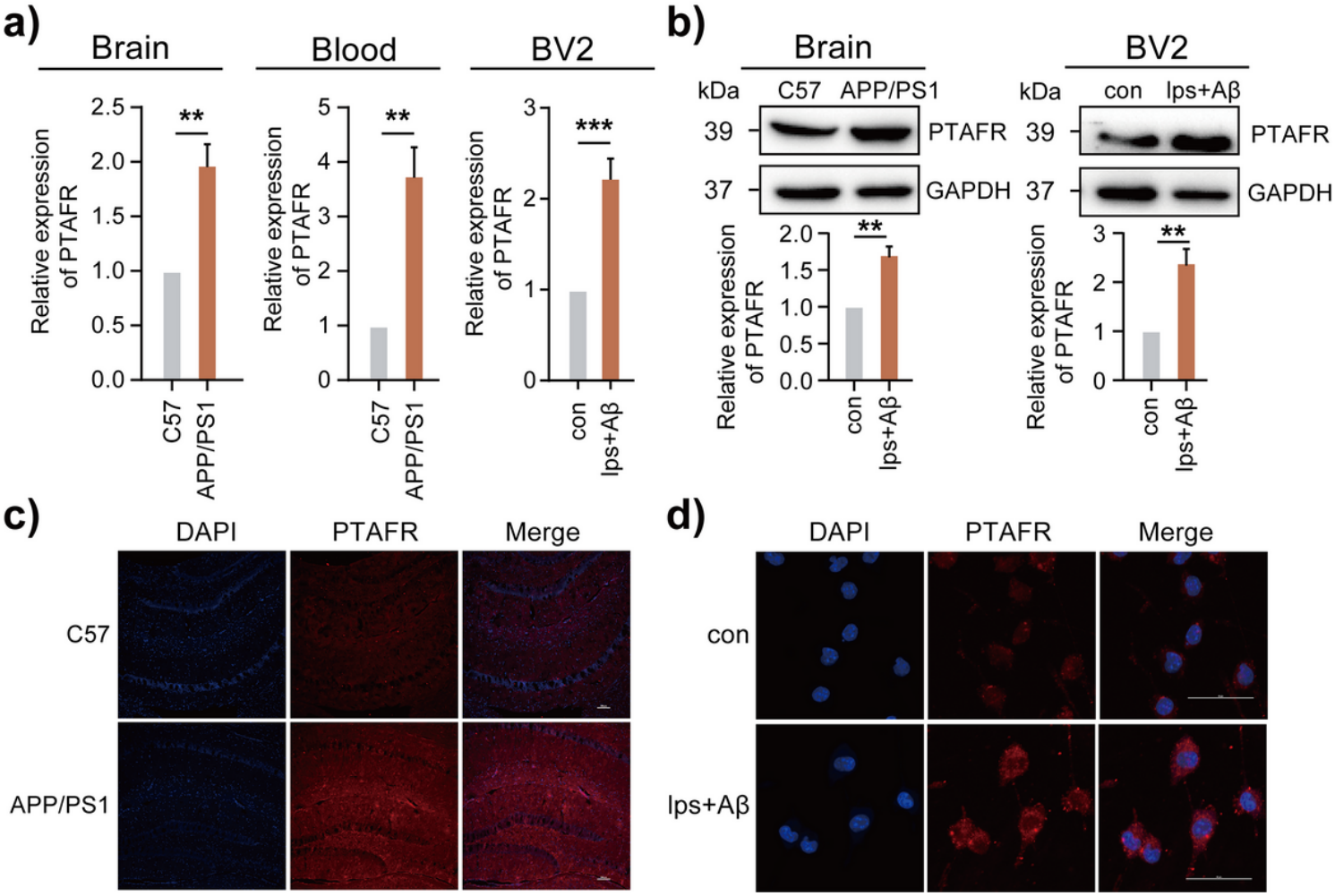

Figure 4

PTAFR was highly expressed in 12-month-old APP/PS1 mice and LPS+Aβ-induced BV2 cells. (a) PTAFR mRNA expressions in the hippocampus, peripheral blood of C57BL/6 and APP/PS1 transgenic mice and LPS+Aβ-induced BV2 cells. (b) The protein levels of PTAFR in the hippocampus of C57BL/6, APP/PS1 mice and LPS+Aβ-induced BV2 cells. (c) The PTAFR expressions in the hippocampus of C57BL/6 and

APP/PS1 mice by immunofluorescence staining. (d) The PTAFR expressions in BV2 cells induced by LPS+Aβ. *P<0.05, **P<0.01, ***P<0.001, ****P<0.001, compared with C57BL/6 group or control group.

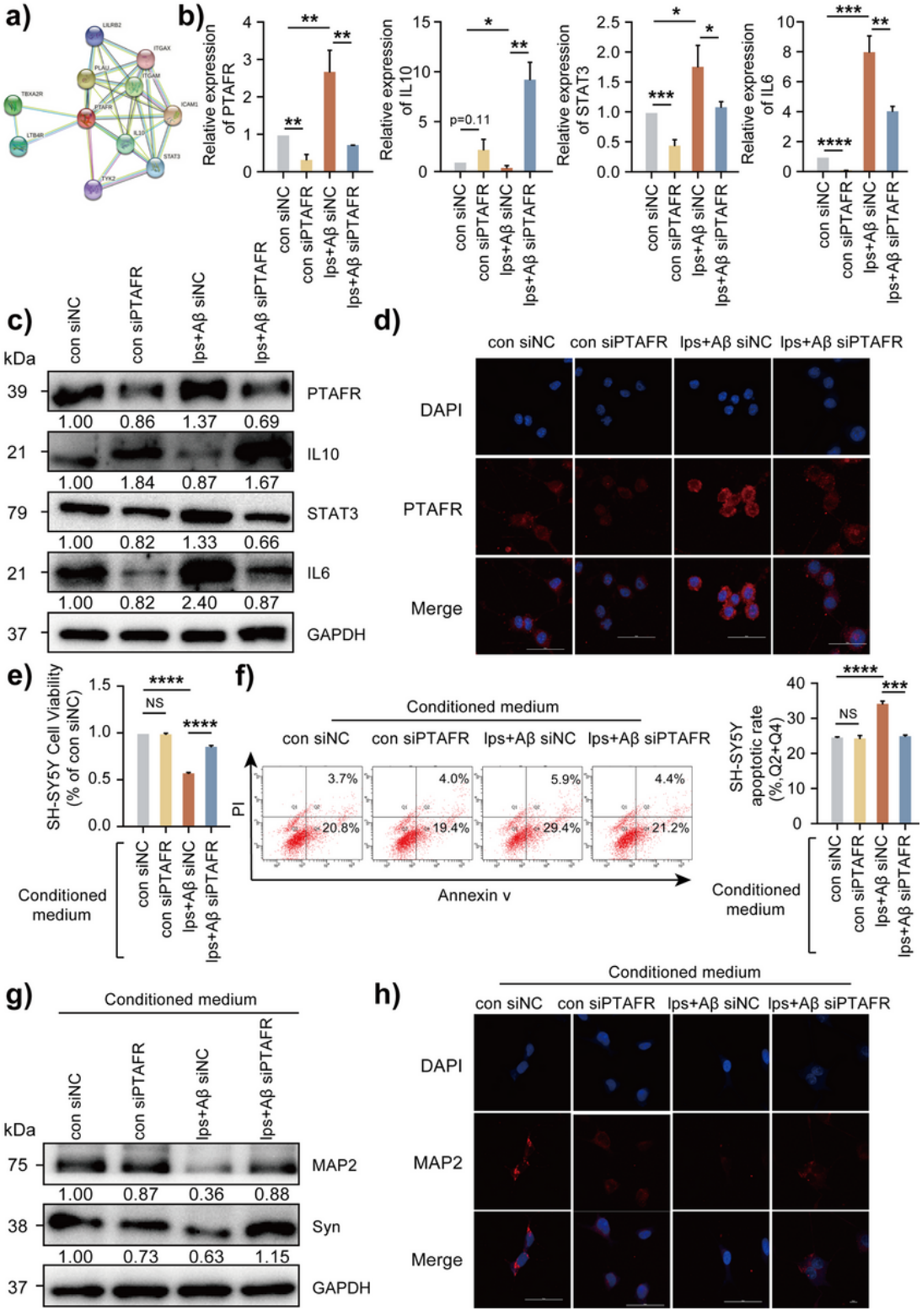

Figure 5

PTAFR exaggerated microglia-mediated microenvironment by increasing the inflammatory factors via IL10-STAT3 signaling. (a) PPI network diagram to predict the possible proteins interacted with PTAFR by STRING online tool. (b) The mRNA expressions of PTAFR, PTAFR, IL10, STAT3, and IL6 in BV2 cells after

silencing. (c) The protein expression levels of PTAFR, IL10, STAT3, and IL6 in BV2 cells after PTAFR was silenced. (d) The immunofluorescence staining of PTAFR (red) and DAPI (blue) in BV2 cells. The conditional medium of BV2 cell was given to SH-SY5Y cells treated with LPS+Aβ. (e) The cell viability of SH-SY5Y cells after CM treatment detected by CCK8 determination, (f) The neuronal apoptosis of SH-SY5Y cells after CM treatment detected by flow cytometry. (g) The expressions of MAP2 and Syn detecting by Western blotting. (h) Immunofluorescence staining of MAP2 (red) and DAPI (blue) in SH-SH5Y cells treated with CM. *P<0.05, **P<0.01, ***P<0.001, ****P<0.001, compared with control group.

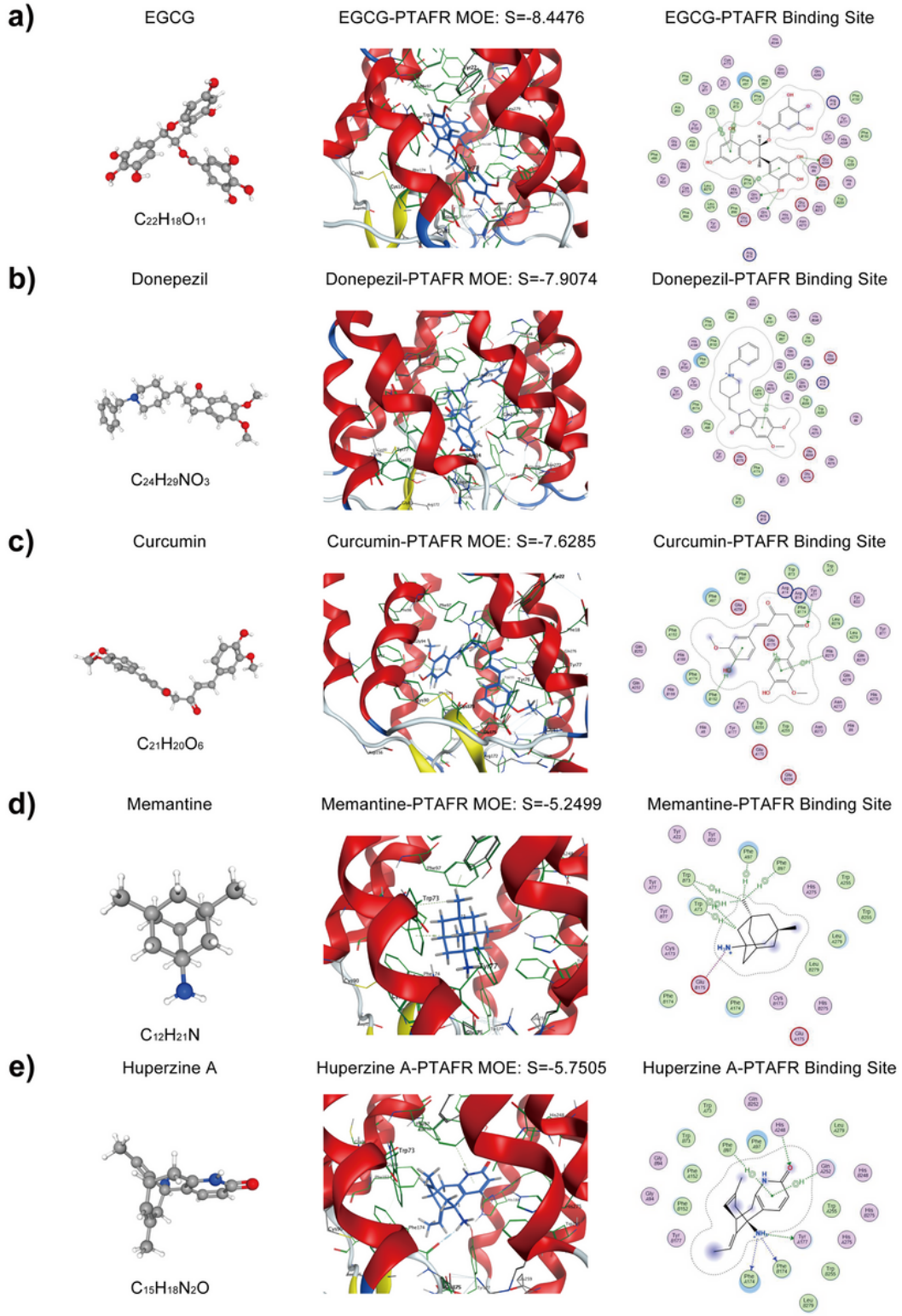

Figure 6

Targeted docking of PTAFR with AD drugs commonly used in clinical practice. (a) (b) (c) (d) (e) are the 3D structures of EGCG, donepezil, curcumin, memantine, and Huperzine A, and their respective binding degrees and binding sites with PTAFR.

Supplementary Files

This is a list of supplementary files associated with this preprint. Click to download.

- FigS1.TIFF.tif
- FigS2.TIFF.tif
- SupplementaryMaterial.pdf